

See discussions, stats, and author profiles for this publication at: <https://www.researchgate.net/publication/280612878>

Synthesis and EPR/UV/Vis–NIR Spectroelectrochemical Investigation of a Persistent Phosphanyl Radical Dication

ARTICLE *in* ANGEWANDTE CHEMIE · JULY 2015

DOI: 10.1002/ange.201502737

READS

63

6 AUTHORS, INCLUDING:



Felix Hennersdorf

Technische Universität Dresden

12 PUBLICATIONS 38 CITATIONS

SEE PROFILE



Evgenia Dmitrieva

Leibniz Institute for Solid State and Materia...

18 PUBLICATIONS 124 CITATIONS

SEE PROFILE



Jan J Weigand

Technische Universität Dresden

99 PUBLICATIONS 1,898 CITATIONS

SEE PROFILE

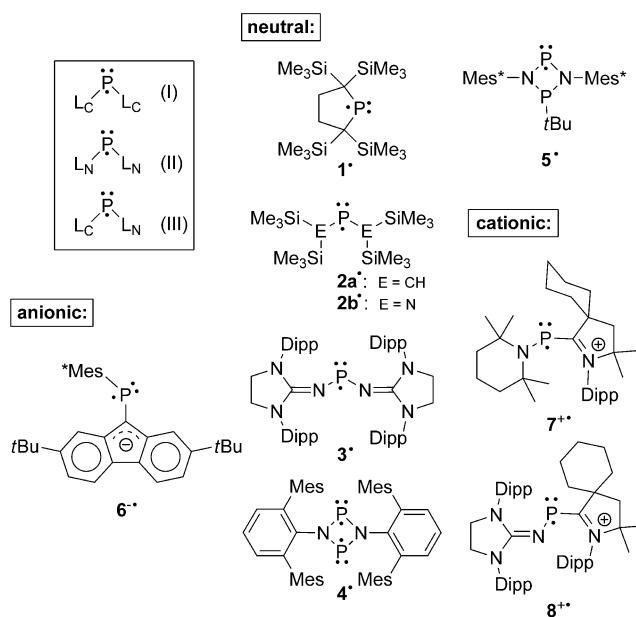
Synthesis and EPR/UV/Vis-NIR Spectroelectrochemical Investigation of a Persistent Phosphanyl Radical Dication

Kai Schwedtmann, Stephen Schulz, Felix Hennersdorf, Thomas Strassner, Evgenia Dmitrieva, and Jan J. Weigand*

Dedicated to Professor Manfred Scheer on the occasion of his 60th birthday

Abstract: The reaction of the bis(imidazoliumyl)-substituted P^I cation $[(2-Im^{Dipp})P(4-Im^{Dipp})]^+$ (10^+) (2-Im = imidazolium-2-yl; 4-Im = imidazolium-4-yl; Dipp = 2,6-di-isopropylphenyl) with trifluoromethanesulfonic acid (HOTf) or methyl trifluoromethylsulfonate (MeOTf) yields the corresponding protonated $[(2-Im^{Dipp})PH(4-Im^{Dipp})]^{2+}$ (11^{2+}) and methylated $[(2-Im^{Dipp})PMe(4-Im^{Dipp})]^{2+}$ (12^{2+}) dications, respectively. EPR/UV/Vis-NIR spectroelectrochemical investigation of the low-coordinated P^I cation 10^+ predicted a stable and “bottleable” P-centered radical dication $[(2-Im^{Dipp})P(4-Im^{Dipp})]^{2+}$ (13^{2+}). The reaction of 10^+ with the nitrosyl salt $NO[OTf]$ yields the persistent phosphanyl radical dication 13^{2+} as triflate salt in crystalline form. Quantum chemical investigation revealed an exceptional high spin density at the P atom.

Among several bonding motifs possible for charged and uncharged P_1 -centered radicals, phosphanyl radicals are particularly intriguing.^[1] Such radicals feature a two-coordinate P atom in the +II oxidation state in combination with either C- (I) or N-based (II)—or a combination of both (III)—substituents L_C or L_N (Scheme 1). Especially low-coordinate P-radical species require stabilization by either bulky substituents (kinetic stabilization), and/or spin delocalization (thermodynamic stabilization).^[2] However, only a few examples are known that are stable enough to be isolated in the solid state. Representative examples of isolated and structurally characterized neutral ($1^{\cdot-}$ – 5^{\cdot}),^[3–6] anionic ($6^{\cdot-}$),^[7] and cationic (7^+ , 8^+)^[8,9] derivatives are depicted in Scheme 1. The stability of the radical cations is also explained by the positive charge leading to electrostatic repulsive effects. Surprisingly, and to the best of our knowledge, no example of a phosphanyl radical dication has been reported



Scheme 1. Structurally characterized phosphanyl radicals.

so far, although with the isolation of radical cations of type 7^+ and 8^+ those species should be feasible. Thus, a dicationic radical species might be accessible by a formal exchange of the L_N substituent in cations of type 7^+ or 8^+ by an imidazoliumyl substituent. Recently, we reported on the high-yielding synthesis of the cationic phosphanide 10^+ , bearing two lone pairs of electrons at the P atom, which we obtained from the reduction of dication 9^{2+} (Scheme 2).^[10] Cation 10^+ is supposed to react with electrophiles such as trifluoromethanesulfonic acid (HOTf) or methyl trifluoromethylsulfonate (MeOTf) to give the respective protonated (11^{2+}) and methylated dications (12^{2+}) as triflate salts, respectively (Scheme 2). The unique combination of the C-bonded N-heterocyclic substituents (L_C) on the two-coordinate phosphorus atom in cation 10^+ makes it an excellent substrate for the synthesis of the hitherto unknown phosphanyl radical dication 13^{2+} (Scheme 2).

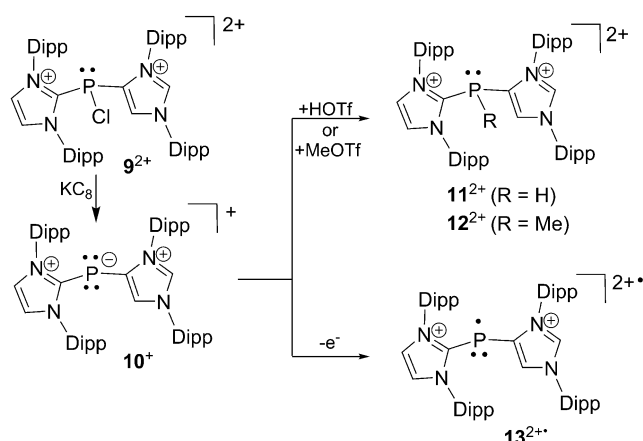
Reacting 10^+ with HOTf or MeOTf in CH_2Cl_2 gives the expected dications 11^{2+} (88 %) and 12^{2+} (83 %) as triflate salts in very good yield (Scheme 2).^[11] Both compounds are obtained as colorless, moisture-sensitive crystalline material.

[*] K. Schwedtmann, S. Schulz, F. Hennersdorf, Prof. Dr. J. J. Weigand
TU Dresden, Professur für Anorganische Molekülchemie
01062 Dresden (Germany)
E-mail: jan.weigand@tu-dresden.de

Prof. Dr. T. Strassner
TU Dresden, Professur für Physikalische Organische Chemie
01062 Dresden (Germany)

Dr. E. Dmitrieva
Leibniz-Institut für Festkörper- und
Werkstoffforschung Dresden, 01069 Dresden (Germany)

Supporting information for this article is available on the WWW
under <http://dx.doi.org/10.1002/anie.201502737>.



Scheme 2. Reaction of cation 10^+ with electrophiles (HOTf, MeOTf) to dications 11^{2+} and 12^{2+} and oxidation to radical dication 13^{2+} .

The ^{31}P NMR spectrum of the purified compound $11[\text{OTf}]_2$ displays a doublet resonance at $\delta = -117.9$ ppm exhibiting an expected $^1J_{\text{PH}}$ coupling constant of 251 Hz.^[12] For compound $12[\text{OTf}]_2$ a quartet resonance is observed at $\delta = -54.4$ ppm with a $^2J_{\text{PH}}$ coupling constant of 9 Hz consistent with a methyl group attached to the three-coordinate P atom. Suitable crystals for X-ray investigation were obtained for compound $11[\text{OTf}]_2$ and the molecular arrangement of cation 11^{2+} is depicted in Figure 1a. As expected,

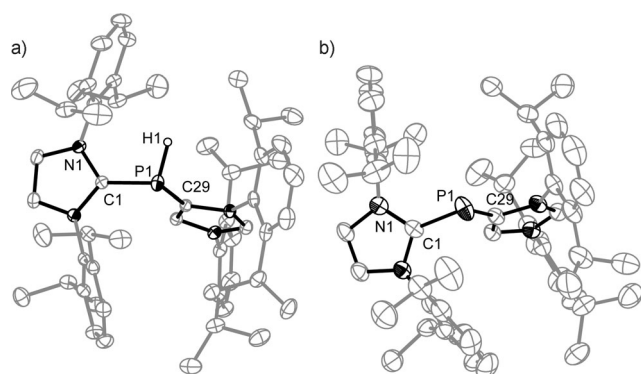
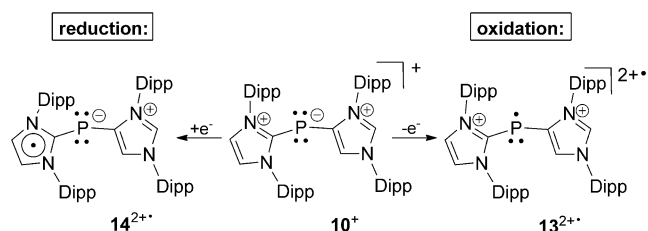


Figure 1. a) Molecular structure of dication 11^{2+} . Selected bond lengths (Å) and angles (°): P1–C1 1.813(3), P1–C29 1.821(2); C1–P1–C29 101.82(10), C1–P1–H1 94.5(14), C29–P1–H1 102.1(14); torsion angle: C29–P1–C1–N1 113.5(2). b) Molecular structure of radical dication 13^{2+} . P1–C1 1.808(4), P1–C29 1.800(4); C1–P1–C29 102.15(16); torsion angle: C29–P1–C1–N1 114.8(3). Solvent molecules anions and carbon bonded hydrogen atoms are omitted for clarity, and thermal ellipsoids are displayed at 50% probability (153 K).

cation 11^{2+} displays a distorted trigonal pyramidal bonding environment around the P atom. The P–C bond lengths (P1–C1 1.813(3) Å, P1–C29 1.821(2) Å) are in the expected range and comparable to those observed for dication 9^{2+} (P1–C1 1.838(3) Å, P1–C29 1.820(2) Å).^[10] In particular, the elongation of the P1–C1 bond length compared to that of 10^+ (P1–C1 1.773(3) Å) is consistent with a lesser degree of π -bonding between C1 and P1. The C1–P1–C29 angle (101.82(10)°) is

slightly narrower compared to C1–P1–C29 (109.2(1)°) of 10^+ , but there is a dramatic difference in the torsion angles for the two cations (11^{2+} : C29–P1–C1–N1 113.5(2)°; 10^+ : C29–P1–C1–N1 170.80(16)°), showing that the imidazoliumyl substituents are substantially twisted in the dicationic structure of 11^{2+} .

Anticipating an interesting reduction/oxidation behavior of cation 10^+ (see Scheme 3) we performed an EPR/UV/Vis-



Scheme 3. Electrochemical reduction of cation 10^+ to unstable neutral radical 14^+ and oxidation to radical dication 13^{2+} .

NIR spectroelectrochemical^[13] investigation to elucidate the possibility for the preparation of stable radicals. The cyclic voltammogram of a solution of $10[\text{OTf}]$ in THF/*n*Bu₄N[OTf] (0.1M) shows one reversible oxidation at $E_{1/2} = 0.22$ V (vs. $E_{1/2}(\text{Fc}/\text{Fc}^+)$) and one irreversible reduction peak at $E_p = -3.06$ V (vs. $E_{1/2}(\text{Fc}/\text{Fc}^+)$; Figure 3a). Peak parameters of the oxidation ($10^+ \rightarrow 13^{2+}$) to radical dication 13^{2+} at given scan rate and their behavior at higher scan rates indicate a reversible electrochemical oxidation.

In contrast to the oxidation the peak shape of the reduction to neutral radical 14^+ is assigned to an electrochemical irreversible reaction or a follow-up reaction (see Figure S3 in the Supporting Information).^[14] The in situ reflective measurement^[15] (Figure S5) of the UV/Vis-NIR spectra of the electrode surface during a cyclic voltammetry (CV) measurement (Figure 2, Vis-CV Figure S6) reveal further insights into the formation of red-colored radical species. The Vis part of the UV/Vis-NIR spectra (x axis) during three cycles of CV measurements of 10^+ is shown and correlated to the time (left y axis) and the potential (right y axis; Figure 2). When the oxidation potential reaches a value of $E > 0.22$ V, radical dication 13^{2+} is formed and its characteristic band at 487 nm can be observed (spectrum at this potential: orange curve, top). Afterwards, radical dication 13^{2+} is reduced back to cation 10^+ (negative peak, right y axis). At comparably strong negative potentials ($E < -3.06$ V) 10^+ is reduced to neutral radical 14^+ (spectrum at this potential: green curve, top). An appearance of the assigned band at 451 nm (see Figure S6) and the disappearance without a peak at the corresponding potential in the current curve of the CV measurement (Figure 3a) can be attributed to a low stability of neutral radical 14^+ . A differentiation between an irreversible electrochemical process and a follow-up reaction is given by CV measurement at high scan rates, where the oxidation peak of 14^+ is observed (see Figure S4).^[16] A more preparative evidence on the stability of radical dication 13^{2+} and instability of 14^+ is given by EPR/UV/Vis-NIR spectro-electrochemistry in thin-layer cells^[17,18]

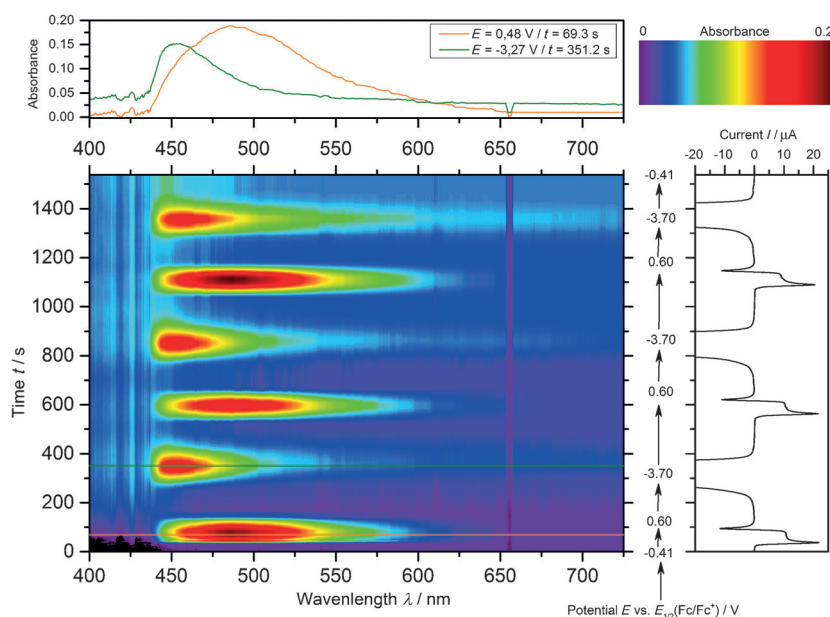


Figure 2. In situ reflective UV/Vis-NIR spectroelectrochemical measurement of a Pt disc electrode surface of a $\text{CH}_2\text{Cl}_2/n\text{Bu}_4\text{N}[\text{OTf}]$ (0.1 M) solution of $10[\text{OTf}]$ (1.3×10^{-3} M) during a cyclic voltammogram ($\nu = 15 \text{ mVs}^{-1}$). Corresponding Vis spectra of formed 13^{2+} (orange curve, top), radical 14^{\bullet} (green curve, top) and current time–potential curve (right).

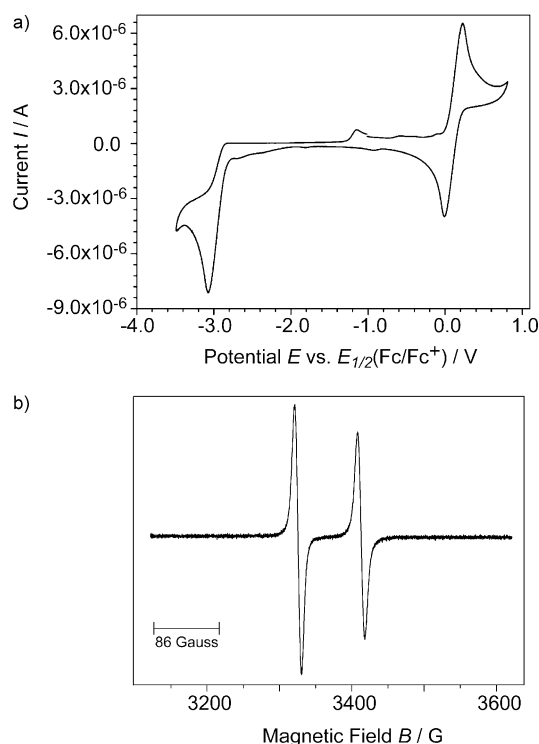
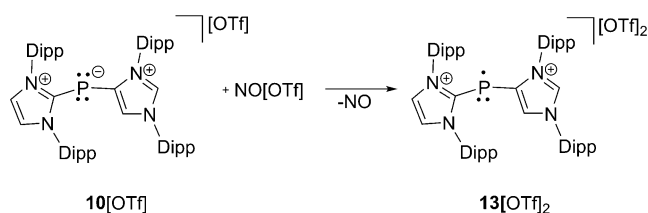


Figure 3. a) Cyclic voltammogram of a $\text{THF}/n\text{Bu}_4\text{N}[\text{OTf}]$ solution of $10[\text{OTf}]$ at a glassy carbon disc electrode. b) EPR spectrum of $13[\text{OTf}]_2$ in $o\text{-C}_6\text{H}_4\text{F}_2$ at ambient temperature.

with complete conversion of the substrate 10^+ . The UV/Vis-NIR-CV measurements show UV/Vis absorptions at 248, 287, 323, 395, and 487 nm for radical dication 13^{2+} accompanied

by the disappearance of the absorption at 418 nm for 10^+ (see Figures S7 and S8). The potential dependencies of the emerging absorption bands and that of the EPR signal are in good agreement (see Figure S9). Contrariwise, no absorptions in the UV/Vis spectra can be observed for the reductive reaction, even at low potentials, indicating the aforementioned low stability of 14^{\bullet} . This result in combination with high-speed CV measurements (see Figure S4), in which the reduction process shows a more reversible character, give evidence for a chemical follow-up reaction of radical 14^{\bullet} . Quantum chemical calculations of 14^{\bullet} have shown that the spin density is to a large extent located at the C2-bound imidazolyl ring (80%; see section S3.7 in the Supporting Information). The results of the spectroelectrochemical investigations forecast the preparative accessibility of stable radical dication 13^{2+} . Thus, reacting $10[\text{OTf}]$ with one equivalent of nitrosyl triflate ($\text{NO}[\text{OTf}]$)^[19] in THF at -78°C leads upon warming to ambient temperature to a deep-red suspension. After workup, the

extremely air- and moisture sensitive P-centered radical dication 13^{2+} was isolated as red powder in good yield as triflate salt (73 %, Scheme 4). The room temperature EPR



Scheme 4. Oxidation of $10[\text{OTf}]$ with $\text{NO}[\text{OTf}]$ to $13[\text{OTf}]_2$ in THF from -78°C to RT.

spectrum of $13[\text{OTf}]_2$ in o -difluorobenzene displays a doublet ($g = 2.006$) due to a large hyperfine coupling constant with the phosphorus nucleus [$a(^{31}\text{P}) = 86 \text{ G}$] (Figure 3b). This hyperfine coupling constant is comparable to those observed for other phosphanyl radicals^[3–9] with a typical range of $a(^{31}\text{P}) = 42\text{--}99 \text{ G}$. Interestingly, no hyperfine coupling is observed to the ^{14}N atoms, indicating that the singly occupied molecular orbital (SOMO) is barely delocalized over the π -conjugated substituents but located primarily at the P atom. Deep-red single crystals, suitable for X-ray diffraction study, were obtained by slow diffusion of n -pentane into a o -difluorobenzene solution of $13[\text{OTf}]_2$ at -35°C .

The molecular structure (Figure 1b) of radical dication 13^{2+} reveals a bent bonding environment at the P atom with a C1–P–C29 angle of $102.15(16)^\circ$. Similar to the molecular structure of dication 11^{2+} the imidazoliumyl substituents are strongly twisted (13^{2+} : C29–P1–C1–N1 $114.8(3)^\circ$). The P1–C1 and P1–C29 bond lengths ($1.808(4) \text{ \AA}$, $1.800(4) \text{ \AA}$) are

elongated, compared to 10^+ , also showing a lesser degree of π bonding between P1 and C1. However, compared to dication 11^{2+} the P–C bond lengths in 13^{2+} are slightly shorter, indicating a partial delocalization of the single electron, which is also shown by the quantum chemical calculations, performed using the Gaussian09 program suite.^[11,20] The density functional theory (DFT) hybrid models B3LYP^[21] and M06^[22] were used together with the 6-31G(d) basis set^[23] for geometry optimizations. The spin density has been calculated by different methods. Both agree that it is largely centered on the P atom and also that it is around 80 % (B3LYP: 79 %; M06: 81 %), consistent with the considerably high spin localization on the P atom observed by EPR spectroscopy. Single-point calculations with different methods based on the B3LYP optimized geometry came to the same results or gave even higher spin densities.^[11] Figure 4

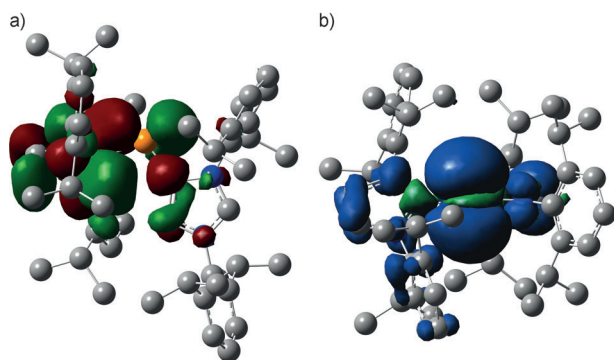


Figure 4. a) Calculated SOMO and b) spin density distribution of radical dication 13^{2+} (B3LYP/6-31G(d); hydrogen atoms are omitted for clarity).

shows the calculated SOMO (left) illustrating that it has primarily p-orbital character and the spin density distribution from the fully optimized B3LYP/6-31G(d) structure of radical dication 13^{2+} (right). The calculated geometrical parameters (C1–P1–C29 104.9°; P1–C1 1.853 Å, P1–C29 1.805 Å; C29–P1–C1–N1 107.8°) are in good agreement with the data from the solid-state structure although there are slight differences within the two imidazolium ring systems. The NBO analysis yielded Wiberg bond indices of 1.0252 and 0.9348 for the P1–C29 and P1–C1 bonds, respectively. The natural bond orbital (NBO) bond order was calculated as 0.8696 (P1–C29) and 0.8197 (P1–C1). The calculated Mulliken and NPA charges are given in the supporting information (see S3.11, SI). The aforementioned results reveal the stability of radical dication 13^{2+} is not only contributed by a thermodynamic stabilization (conjugated π system) but more by kinetic stabilization (bulky substituents, charge repulsion).

In summary, we illustrated that the two-coordinate P^I cation (10^+) readily reacts with HOTf or MeOTf to give the corresponding protonated (11^{2+}) and methylated (12^{2+}) dications, respectively. In-depth EPR/UV/Vis-NIR spectroelectrochemical investigations of 10^+ revealed two radical species 14^{\cdot} by electrochemical reduction, and 13^{2+} by electrochemical oxidation, whereat the latter was predicted to be persistent in solution and the solid state. The reaction of

10^+ with nitrosyl triflate leads to the formation of the remarkable and stable phosphanyl radical dication 13^{2+} showing a high spin density at the P atom. This work shows the accessibility of a stable phosphanyl radical dication, namely 13^{2+} , and extends the already existing set of intriguing phosphanyl radical species (Scheme 1).

Acknowledgements

This work was supported by the Fonds der Chemischen Industrie (FCI, Kekulé scholarship for F.H.) and the German Science Foundation (DFG, grant number WE 4621/2-1) and the ERC (grant number SynPhos 307616). We thank the Center for Information Services and High Performance Computing (ZIH) for the generous allocation of computation time.

Keywords: dications · EPR spectroscopy · phosphorus · radicals · spectroelectrochemistry

- [1] For reviews see: a) A. Armstrong, T. Chivers, R. T. Boere, *ACS Symp. Ser.* **2006**, 917, 66; b) S. Marque, P. Tordo, *Top. Curr. Chem.* **2005**, 250, 43; c) P. P. Power, *Chem. Rev.* **2003**, 103, 789; d) M. Geoffroy, *Recent Res. Dev. Phys. Chem. Solids* **1998**, 2, 311; e) M. D. Caleb, M. Soleilhavoup, G. Bertrand, *Chem. Sci.* **2013**, 4, 3020, and references therein.
- [2] a) P. Agarwal, N. A. Piro, K. Meyer, P. Muller, C. C. Cummins, *Angew. Chem. Int. Ed.* **2007**, 46, 3111; *Angew. Chem.* **2007**, 119, 3171; b) A. Armstrong, T. Chivers, M. Parvez, R. T. Boere, *Angew. Chem. Int. Ed.* **2004**, 43, 502; *Angew. Chem.* **2004**, 116, 508; c) S. Ito, M. Kikuchi, M. Yoshifuji, A. J. Arduengo III, T. A. Konovalova, L. D. Kispert, *Angew. Chem. Int. Ed.* **2006**, 45, 4341; *Angew. Chem.* **2006**, 118, 4447; d) M. Scheer, C. Kuntz, M. Stubenhofer, M. Linseis, R. F. Winter, M. Sierka, *Angew. Chem. Int. Ed.* **2009**, 48, 2600; *Angew. Chem.* **2009**, 121, 2638.
- [3] S. Ishida, F. Hirakawa, T. Iwamoto, *J. Am. Chem. Soc.* **2011**, 133, 12968.
- [4] a) S. L. Hinchley, C. A. Morrison, D. W. H. Rankin, C. L. B. Macdonald, R. J. Wiacek, A. H. Cowley, M. F. Lappert, G. Gundersen, J. A. C. Clyburne, P. P. Power, *Chem. Commun.* **2000**, 2045; b) S. L. Hinchley, C. A. Morrison, D. W. H. Rankin, C. L. B. Macdonald, R. J. Wiacek, A. Voigt, A. H. Cowley, M. F. Lappert, G. Gundersen, J. A. C. Clyburne, P. P. Power, *J. Am. Chem. Soc.* **2001**, 123, 9045; c) J. P. Bezombes, K. B. Borisenko, P. B. Hitchcock, M. F. Lappert, J. E. Nycz, D. W. H. Rankin, H. E. Robertson, *Dalton Trans.* **2004**, 1980.
- [5] O. Back, B. Donnadieu, M. von Hopffgarten, S. Klein, R. Tonner, G. Frenking, G. Bertrand, *Chem. Sci.* **2011**, 2, 858.
- [6] T. Beweries, R. Kuzora, U. Rosenthal, A. Schulz, A. Villinger, *Angew. Chem. Int. Ed.* **2011**, 50, 8974; *Angew. Chem.* **2011**, 123, 9136.
- [7] X. Pan, X. Wang, Y. Zhao, Y. Sui, X. Wang, *J. Am. Chem. Soc.* **2014**, 136, 9834.
- [8] O. Back, M. A. Celik, G. Frenking, M. Melaimi, B. Donnadieu, G. Bertrand, *J. Am. Chem. Soc.* **2010**, 132, 10262.
- [9] R. Kinjo, B. Donnadieu, G. Bertrand, *Angew. Chem. Int. Ed.* **2010**, 49, 5930; *Angew. Chem.* **2010**, 122, 6066.
- [10] K. Schwedtmann, M. H. Holthausen, K.-O. Feldmann, J. J. Weigand, *Angew. Chem. Int. Ed.* **2013**, 52, 14204; *Angew. Chem.* **2013**, 125, 14454.

- [11] See supporting information for further details.
- [12] O. Kühl, *Phosphorus-31 NMR Spectroscopy*, Springer, Berlin, **2008**.
- [13] a) W. Kaim, J. Fiedler, *Chem. Soc. Rev.* **2009**, 38, 3373; b) W. Kaim, A. Klein, *Spectroelectrochemistry*, Royal Society of Chemistry, Cambridge, **2008**, and references therein; c) A. Petr, L. Dunsch, A. Neudeck, *J. Electroanal. Chem.* **1996**, 412, 153; d) L. Dunsch, *J. Electroanal. Chem.* **1975**, 61, 61.
- [14] J. Heinze, *Angew. Chem. Int. Ed. Engl.* **1984**, 23, 831; *Angew. Chem.* **1984**, 96, 823.
- [15] a) U. Schroeder, F. Scholz, *J. Solid State Electrochem.* **1997**, 1, 62; b) F. Scholz, *Electroanalytical Methods*, Springer, Berlin, **2002**.
- [16] a) J. M. Saveant, *Electrochim. Acta* **1967**, 12, 999; b) R. S. Nicholson, I. Shain, *Anal. Chem.* **1964**, 36, 706.
- [17] J. Niu, S. Dong, *Rev. Anal. Chem.* **1996**, 15, 1.
- [18] a) R. W. Murray, W. R. Heinemann, G. W. O'Dom, *Anal. Chem.* **1967**, 39, 1666; b) T. P. DeAgelis, W. R. Heineman, *J. Chem. Educ.* **1967**, 44, 594.
- [19] The synthesis of nitrosyl triflate was carried out according to a literature procedure: R. Weiss, K.-G. Wagner, *Chem. Ber.* **1984**, 117, 1973.
- [20] M. L. Frisch; Gaussian 09, Revision A.02, Gaussian, Inc., Wallingford CT, **2009**; for a complete list of authors see the Supporting Information.
- [21] a) A. D. Becke, *J. Chem. Phys.* **1993**, 98, 5648; b) C. Lee, W. Yang, R. G. Parr, *Phys. Rev. B* **1988**, 37, 785; c) P. J. Stephens, E. J. Devlin, C. F. Chabalowski, M. J. Frisch, *J. Phys. Chem.* **1994**, 98, 11623; d) S. H. Vosko, L. Wilk, M. Nusair, *Can. J. Phys.* **1980**, 58, 1200.
- [22] a) Y. Zhao, D. G. Truhlar, *Theor. Chem. Acc.* **2008**, 119, 525; b) Y. Zhao, D. G. Truhlar, *Theor. Chem. Acc.* **2008**, 120, 215.
- [23] a) W. J. Hehre, R. Ditchfield, J. A. Pople, *J. Chem. Phys.* **1980**, 72–73, 2257; b) M. M. Francl, W. J. Pietro, W. J. Hehre, J. S. Binkley, M. S. Gordon, D. J. DeFrees, J. A. Pople, *J. Chem. Phys.* **1982**, 77, 3654; c) R. C. Binning, Jr., L. A. Curtiss, *J. Comput. Chem.* **1990**, 11, 1206.

Received: March 24, 2015

Published online: ■ ■ ■ ■, ■ ■ ■ ■

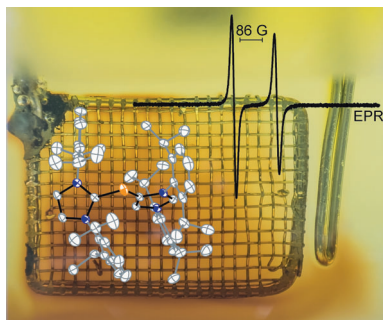
Zuschriften



Phosphorradikal

K. Schwedtmann, S. Schulz,
F. Hennesdorf, T. Strassner,
E. Dmitrieva,
J. J. Weigand* ————— ■■■■-■■■■

Synthesis and EPR/UV/Vis-NIR
Spectroelectrochemical Investigation of
a Persistent Phosphanyl Radical Dication



Stabiles Phosphor-Radikal: Die Reaktion eines Bis(imidazoliumyl)-substituierten, zweifach koordinierten P^I -Kations mit Trifluormethansulfonsäure oder Methyltrifluormethylsulfonat ergibt das entsprechende protonierte oder methylierte Dikation. Spektroelektrochemische EPR/UV/Vis-NIR-Studien dieses P^I -Kations verweisen auf die Bildung einer stabilen Radikalspezies (siehe Bild).